Nanoscale

Accepted Manuscript

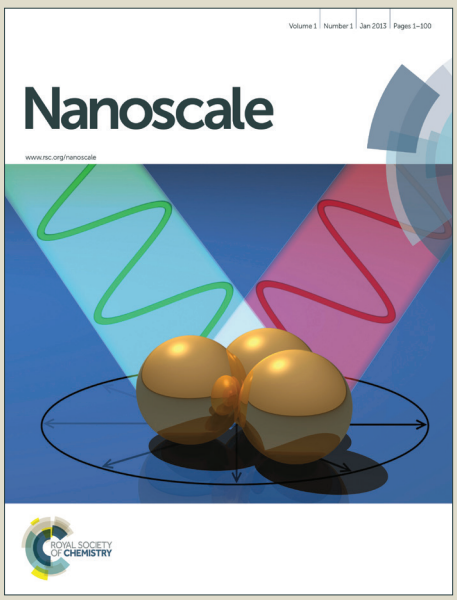

ROYAL SOCIETY OF CHEMISTRY

www.rsc.org/nanoscale

Nanoparticle-Coated Micro-Optofluidic Ring Resonator as a Detector for Microscale Gas Chromatographic Vapor Analysis

K. W. Scholten,[a,e] W. R. Collin,[b,e] X. Fan,[c,e] and E. T. Zellers[a,b,e*]

[a]Applied Physics Program, University of Michigan, Ann Arbor, MI, USA 48109-1040

[b] Department of Chemistry, University of Michigan, Ann Arbor, MI, 48109-1055

[c]Department of Biomedical Engineering, University of Michigan, Ann Arbor, MI, 48109- 2110

[d] Department of Environmental Health Sciences, Univ. of Michigan, Ann Arbor, MI 48109-2029

[e] Center for Wireless Integrated MicroSensing and Systems (WIMS^2), University of Michigan, Ann Arbor, MI, 48109-2122

Abstract

A vapor sensor comprising a nanoparticle-coated microfabricated optofluidic ring resonator (μOFRR) is introduced. A multilayer film of polyether functionalized thiolate monolayer protected gold nanoparticles (MPN) was solvent cast on the inner wall of the hollow cylindrical SiO_x μOFRR resonator structure, and whispering gallery mode (WGM) resonances were generated with a 1550-nm tunable laser via an optical fiber taper. Reversible shifts in the WGM resonant wavelength upon vapor exposure were detected with a photodetector. The μOFRR chip was connected to a pair of upstream etched-Si chips containing PDMS-coated separation μcolumns and calibration curves were generated from the peak-area responses to five volatile organic compounds (VOCs). Calibration curves were linear, and the sensitivities reflected the influence of analyte volatility and analyte-MPN functional group affinity. Sorption-induced changes in film thickness apparently dominate over changes in the refractive index of the film as the determinant of responses for all VOCs. Peaks from the MPN-coated μOFRR were just 20-50% wider than those from a flame ionization detector for similar μcolumn

separation conditions, reflecting the rapid response of the sensor for VOCs. The five VOCs were baseline separated in < 1.67 min, with detection limits as low as 38 ng.

Introduction

Films of thiolate-monolayer-protected gold nanoparticles (MPN) have been used as sorptive interface layers for vapor sensing with chemiresistors,[1-4] thickness-shear-mode resonators,[5-8] and optical sensors of various designs.[9-14] The extinction (i.e., absorbance and scattering) of visible light by MPN films is influenced by a localized surface plasmon resonance (LSPR) arising from the interaction of the incident light with free electrons on the surfaces of the gold nanoparticle cores. At a given wavelength, the net extinction is affected by a number of variables, including the size, shape, packing order and separation of the metal core, and the refractive index (RI) of the inter-core matrix.[15] Sorption of volatile organic compounds (VOC) into the thiolate monolayers comprising the inter-core matrix of MPN films can change the thickness, inter-core spacing, and RI of the MPN film. The resulting changes in extinction can be measured and related to the gas-phase VOC concentration. [9,13,14]

In previous studies of optical vapor sensing with MPN films, light signals were measured with spectrophotometers through free space during exposure of the films to VOCs.[9-11,13,14] A similar approach was used for gas and VOC sensing with surface-immobilized gold nano-islands coated with a polymer film.[16-18] Chen et al. adapted this approach to create a nanoparticle-lined microfluidic capillary, that they then installed as a detector downstream from a conventional gas chromatographic (GC) column.[12] In most such studies, sensitivities to the VOC analytes tested were rather low, leading to relatively high limits of detection (LOD). Additionally, none of the configurations employed is well suited for miniaturization or integration into gas

chromatographic microsystems (μGC) for analysis of VOC mixtures. Several other optical vapor sensors have been reported that also require through-space transmission of light, some of which are more suitable for μGC integration and/or can achieve lower LODs by exploiting phenomena such as Fabry-Perot resonance.[19,20]

The optofluidic ring resonator (OFRR) is a unique optical sensing platform in which vapor sensing and fluidic transport functions are combined.[21,22] Whispering gallery modes (WGMs) are generated in the wall of a glass capillary by a proximal optical fiber taper, and the evanescent component of the WGM probes the inner surface of the OFRR capillary. By scanning the laser wavelength and monitoring the output intensity across the waveguide a resonant wavelength (λ_{WGM}) can be identified as the wavelength of minimum output. Any change in the optical properties (such as *RI*) near the surface causes a shift in λ_{WGM}, which serves as a sensor response.

The first reported OFRR sensors were fabricated from heat-drawn glass capillaries that were etched to further thin the walls, and then lined with sorptive polymer films.[21-23] Shifts in λ_{WGM} would arise from changes in the polymer film thickness and/or *RI* accompanying reversible partitioning of vapor-phase VOC analytes flowing through the capillary. With inner diameters ≤ 100 μm, such OFRRs could serve as sensitive GC detectors for VOC mixtures.[23] However, such devices are not suitable for microsystem integration because they are fragile, cumbersome, and not amenable to precise batch fabrication.

We recently introduced a *microfabricated* optofluidic ring resonator (μOFRR) and characterized its performance, with a PDMS wall coating, as a detector downstream from conventional and microfabricated GC (μGC) separation columns.[24,25] Resonator structures in these devices are SiO_x cylinders ~80 μm tall with inner diameters ranging from 50-250 μm and

wall thicknesses ≤ 2 μm after partial release from the Si substrate on which they are grown. Best results were obtained using devices with quasi-toroidal expansions in the midsection of the cylinder. WGMs could be excited in the wall of this expansion section by coupling a modulated laser signal via a proximal optical fiber taper, and the resonant wavelengths could be identified as the minima in output intensity across the fiber. Given the high sensitivities and rapid responses to VOCs that we obtained with a PDMS-coated μOFRR,[25] it was of interest to explore whether an MPN-coated device might afford similar performance, with the added prospect of (eventually) imparting selectivity by virtue of the wavelength dependence of VOC responses afforded by such plasmonic interface films.[9-11,13,26]

Here we report first results from an MPN-coated μOFRR probed at a single wavelength and used as a μGC detector. Following a brief description of initial failed attempts to obtain vapor responses from drawn-capillary OFRR and μOFRR devices coated with one type of MPN, we present calibrated vapor responses from a μOFRR device coated with an alternative MPN material. The analysis of a 5-component VOC mixture is then demonstrated with the mounted device connected downstream from a μGC separation module. Results are assessed with respect to the nature of the vapor-MPN interactions, the variables affecting responses, and the prospects for selective, multi-wavelength sensing.

Experimental methods

Materials

Octane-thiolate (C8) MPNs were taken from existing stocks, which were synthesized according to the method of Rowe et al.[27] with a Au core diameter of 4.3 ± 0.9 nm. MPNs containing thiolate monolayers derived from 1-mercapto-(triethylene glycol) methyl ether (TEG) were purchased from Nanoprobes (Yaphank, NY) and had a reported diameter of 5.16 ± 0.89

nm. The test compounds, isopropyl alcohol (IPA), heptane (HEP), toluene (TOL), perchloroethylene (PCE), ethylbenzene (ETB), and all organic solvents were used as received (99%, Sigma Aldrich, St. Louis, MO). Relevant physical properties of the test compounds are given in Table 1.

Drawn-capillary OFRR

Drawn-capillary OFRRs, each consisting of a thinned, fused silica capillary (~50 μm i.d. and 55 μm o.d.) 3 cm in length, were prepared as described previously.[21,23] Each end was inserted into a 10-cm segment of a wider-bore fused silica capillary (155 μm i.d. and 360 μm o.d.) and sealed with adhesive (Hysol Epoxy Patch 1C, Rocky Hill, CT). The thinned capillary was stretched taut between two posts mounted on a metal base plate and fixed in position with double-sided tape. A static coating method[28] was adapted to deposit an MPN film on the interior wall of the OFRR: the thinned capillary was filled with a 24 mg mL^{-1} solution of C8 in 1:1 hexane:dichloromethane, the distal end of the capillary was sealed with paraffin wax and suction pressure of 21 kPa was applied to the proximal end until the solvent had evaporated. N_2 gas was subsequently passed through the capillary for several hours to drive off any residual vapor. Assuming uniform, conformal deposition of the MPNs in solution on the internal surface area of the resonator, and a film density of 4.3 g cm^{-3},[8] the film thickness was estimated to be ~70 nm.

μOFRR

The design and fabrication of the μOFRR has been described.[24,25] The device comprises a hollow SiO_x cylinder with a 250 μm i.d. and 1.2 μm thick walls, partially released from a Si substrate. The μOFRR is located in the center of a 2 × 2 cm chip and provides a fluidic circuit from the top side to the underside. Along the underside of the chip is a plasma etched

microfluidic channel that, once sealed (see below), connects the central μOFRR aperture to an expansion port at the edge of the chip. An etched channel running laterally across the top side of the chip facilitates alignment of a thinned fiber waveguide for coupling to the resonator. Figure 1 shows an illustration and photograph of the packaged sensor chip, and an SEM image of the μOFRR.

A C8 MPN film was deposited on the interior of a μOFRR device by adapting the procedure described in ref. 25 for deposition of PDMS films. The front-side aperture of the (inverted) resonator was sealed by pressing it gently into a soft rubber septum, and the cylinder was filled with a solution of C8 in toluene (2.5 mg mL^{-1}). The device was placed in a chamber under mild vacuum to evaporate the solvent. The presence of the MPN film on the interior of the device was confirmed with optical microscopy. The average MPN film thickness was estimated to be ~100 nm.

To deposit a TEG MPN layer on the inner wall of the μOFRR cylinder, 5 μL of a 2 mg mL^{-1} solution of TEG in ethanol was cast over the underside port of the inverted μOFRR chip by syringe. The solution filled the resonator cylinder and was retained by surface tension at the μOFRR aperture. The solvent was allowed to slowly evaporate under ambient conditions. Values for density of the TEG film were not available, but assuming the same density as C8 and no loss of material, film thickness was estimated to be ~80 nm.

The fluidic channel etched along the backside of μOFRR chip was sealed with a 2 × 2 cm Pyrex cover plate using UV curable glue (NOA 81, Norland Optical, Cranbury, NJ). A short section of fused-silica capillary (250 μm i.d.) was inserted into the expansion port and sealed with Hysol epoxy for external fluidic connection.

Sensor characterization tests

WGM resonances were excited within the walls of both types of devices by coupling light from a tunable laser via an optical fiber waveguide (λ = 980 nm for the OFRR, λ = 1550 nm for the μOFRR).[22,24,25] The source wavelength was varied over a range of several hundred pm by modulating a voltage signal sent to the laser controller by a DAQ card controller, while the output intensity across the fiber was measured with a IR photoreceiver (Model 2033, New Focus, Irvine, CA) and recorded by customized LabVIEW software. λ_{WGM} and full width at half maximum (FWHM) for observed WGMs were calculated using ORIGIN® software (OriginLab Corp., Northampton, MA). During testing, the coated OFRR was mounted to an optics table and the inlet was connected to the heated injection port of a bench-scale gas chromatograph (3800, Varian, Inc., Palo Alto, CA) by a 1-m-long segment of uncoated deactivated fused silica capillary. Helium was used as the carrier gas at flow rates ranging from 1-3 mL/min. The resonant wavelength of each detected WGM was monitored during injections of saturated headspace or neat liquid samples of the VOC analytes.

The coated μOFRR chip was connected by a short segment of deactivated fused silica capillary to two series-coupled, 3-m long microfabricated separation columns (μcolumn) with wall coatings of PDMS. The μcolumns consisted of square spiral channels deep reactive ion etched in Si (3.1 × 3.1 cm chips), an anodically bonded glass cover plate, and platinum resistive heaters and a temperature sensor patterned on the Si.[28,29] The μcolumns were held at 40 °C using the on-chip resistive heaters, and the μOFRR was left at room temperature (~22 °C).

Test atmospheres containing a mixture of the five VOCs were prepared in 3-L Tedlar® bags in an atmosphere of clean, dry air. Four test atmospheres were prepared spanning a 10-fold range in concentrations for all analytes. Aliquots of each test atmosphere were drawn through a

100 µL sample loop and injected by way of a six-port valve into the first µcolumn for separation in a carrier stream of dry air at 2.0 mL min^{-1}. Each analysis was repeated five times. A single WGM resonance was recorded at a rate of 16.7 Hz, and λ_{WGM} was monitored during all exposures. Retention times, peak widths, and peak areas were analyzed with ORIGIN® software.

Results and discussion

OFRR

Numerous closely spaced resonances were measured with the C8-coated OFRR, with Q-factors (λ_{WGM}/FWHM) of ~10^5, comparable to those reported for uncoated and polymer coated drawn-capillary OFRRs.[21-23] However, no shift in λ_{WGM} was ever observed during exposures to VOCs. Optical microscopic inspection of the C8-coated OFRR revealed the coating thickness to be quite variable (Figure 2). We hypothesized that the heterogeneity or surface roughness of the MPN film was scattering light at the inner surface of the OFRR and degrading the modes with evanescent fields that were probing the film. The resonant modes detected were apparently confined to either the bulk or exterior of the OFRR wall. Several aspects of the deposition process were varied in an attempt to create a more uniform film, including changing the casting solvent and C8 concentration, pretreating the surface with HMDS prior to film deposition, and using a water bath to thermostat the OFRR during coating. None of these efforts produced significant changes in film uniformity or yielded responsive MPN-coated OFRR sensors.

µOFRR

Repeated attempts to generate measurable WGM resonances in the µOFRR device after coating with C8 also failed. Although difficult to observe microscopically, the films appeared

non-uniform on this device as well. Therefore, on the basis of a report by Potyrailo et al. that MPNs with TEG monolayers afforded continuous spin-coated films,[9] attempts were made to create a working μOFRR sensor with a TEG film. During initial optical characterization of a TEG-coated device, no WGM resonances could be detected. Then, a 5-μL drop of neat ethanol was placed on the backside port, filling the (inverted) resonator and re-dissolving the TEG. Subsequent evaporation and re-deposition of the TEG film yielded stable, detectable WGM resonances. Figure 3 shows the resonant signal, which has a Q factor of ~8,000. This Q-factor is lower than the those of resonances in uncoated and PDMS-coated devices, which were measured as ~12,000,[24,25] but it is sufficient for VOC sensing.

The success of this approach was likely due to a combination of factors. If TEG formed a more uniform and contiguous film than did C8, then scattering losses thought to be responsible for the failure to create working C8-coated devices would have been reduced: the need to redeposit the original TEG film confirms that resonance can be lost by relatively small changes in film morphology, and that a uniform film is not guaranteed even with this type of MPN. Differences in device geometry may also have played a critical role: the μOFRR expansion region confines a single WGM within a small area on the inner wall of the μOFRR cylinder, which would then reduce the film volume being probed and the likelihood of encountering non-uniformities that might give rise to scattering. Differences in cavity volume and deposition method would also have affected the solvent evaporation rate and, thereby, the quality of the film.[30] The excitation wavelength employed may also have been important: the use of a longer wavelength (i.e., 1550 nm vs. 980 nm) would reduce the degree of light absorbance by the MPN film as well as the degree of scattering by residual surface or film roughness.

MPN-coated μOFRR as μGC detector

During exposure to every VOC λ_{WGM} increased (i.e., red-shifted). Responses were rapid and completely reversible under a flow of dry-air carrier gas. Figure 3 displays a representative shift in λ_{WGM} due to VOC sorption into the TEG film. Red shifts in λ_{WGM} could arise from increases in either the *RI* or thickness of the film, or both.[25] Swelling of MPN films during VOC exposure is well-documented.[1,8,30,31] Reported changes in the optical properties of MPN films due to VOC sorption have been ascribed to an increase in inter-core spacing, alteration of core packing order, and/or changes in the *RI* of the inter-core medium due to differences in the *RI* values of the analyte and monolayer matrix.[9-11,13,14,30,32]

Kubo, et al.[33] modeled changes in the *RI* of Au nanoparticle dispersions in organic media at Au-organic volume fractions similar to the Au-monolayer volume fractions in typical MPN films.[8,21] According to their model, the *RI* in the infrared should increase with the volume fraction of the nanoparticles and should also increase with the dielectric constant of the organic matrix in which the nanoparticles are dispersed. Thus, sorption of VOCs with *RI* values greater than that of the TEG monolayer should increase the film *RI*, and vice-versa, while film swelling, alone, should decrease the film *RI*. This assumes that there is negligible absorbance by the monolayer and VOC, and that the dielectric constant of each constituent can be represented by the square of its *RI* value, both of which are valid assumptions.

Unfortunately, the *RI* value of the TEG MPN has not been reported. Assuming that the *RI* value of the TEG monolayer can be approximated by that of a structural analogue, triethylene glycol monomethyl ether (i.e., 1.439),[34] then it is bracketed by the *RI* values of the VOC analytes tested here, with most VOC *RI* values being lower (see Table 1). This suggests that VOC sorption should decrease the *RI* of the film in most cases, due to a combination of increased

inter-core spacing and decreased *RI* of the inter-core matrix. These changes would lead to blue shifts in λ_{WGM}. The consistent observation of red shifts in λ_{WGM} indicates that responses are instead dominated by swelling-induced increases in MPN film thickness and the consequent increase in the proportion of the evanescent WGM field within the MPN film. Similar results were observed with a PDMS-coated μOFRR also operating in such a thin-film regime (i.e., where the film thickness was less than the evanescent wavelength probing the film).[25] This, in turn, suggests that both the sensitivity and selectivity of responses at this wavelength are dictated by the extent of partitioning and the efficiency of film swelling associated with the sorbed volume of each analyte vapor.[8]

Figure 4 shows a representative chromatogram from the TEG-coated μOFRR installed as the μGC detector. All five compounds eluted within 100 s and were well separated (note: faster separations could easily be achieved), however, IPA consistently co-eluted with a peak that was subsequently determined to be due to water vapor, which is capable of permeating through the walls of the Tedlar bags from the ambient (note: separate tests confirmed that the TEG-coated μOFRR was quite sensitive to water vapor accordant with the polar nature of the polyether monolayer). Average peak widths, taken as the FWHMs, are given in Table 1. They ranged from 0.83 s (IPA) to 3.3 s (ETB) for the largest injections, with RSDs ranging from 3-10% for 5 replicates. The observed increase in FWHM values with decreasing analyte vapor pressure can be ascribed to the increased retention time and the commensurate increase in on-column band broadening, as well as the decreased rate of desorption from the TEG MPN film. Reference chromatograms collected with an FID in place of the μOFRR, which are subject only to on-column band broadening (note: the FID is considered a "zero-dead volume" detector) yielded FWHM values for the same VOCs consistently 1.2-1.5 times smaller than values collected with

the μOFRR (Table 1). Since any column related factors were common to both detectors, the broader μOFRR peaks reflected the finite sorption-desorption rates in-out of the TEG film. These FWHM values are ~3-fold larger than those reported for a somewhat similar set of VOCs detected with PDMS-coated μOFRR,[25] due, primarily, to the shorter μcolumn (i.e., 3 m) used, which yielded retention times ~3-fold shorter. Thus, response speed appears to be comparable between the PDMS- and MPN-coated devices, notwithstanding possible differences in film thicknesses.

The average responses to each vapor were evaluated using the peak areas, which are plotted against the estimated injected masses in Figure 5a (note: the IPA peak areas were corrected for the presence of water vapor by subtraction of the latter, determined from blank analyses, prior to integration). The calibration data were described well by linear regressions with forced-zero y-intercepts (R^2 > 0.966 in all cases), despite the lack of reference data confirming the test-atmosphere concentrations, and somewhat variable responses at a given concentration (i.e., avg. RSD ≅ 16%).

Figure 5b presents a bar chart of the μOFRR sensitivities, taken as the slopes of the calibration lines. The order of sensitivities was ETB>TOL>PCE~IPA>HEP. That the highest sensitivity was found for ETB is consistent with its low vapor pressure (Table 1), which plays a dominant role in the degree of partitioning of VOCs into sorptive interface layers.[35] However, other factors also affected the sensitivities: the sensitivity to IPA was higher than expected and the sensitivity to PCE was slightly lower than would be expected based upon vapor pressure alone.

Figure 5c presents vapor-pressure normalized sensitivities, which reflect the influence of functional group interactions on the sensitivities quite clearly. The relatively high sensitivity for

IPA is consistent with its high polarity and consequent affinity for the polar ether groups in the TEG monolayer. The low sensitivity for HEP is consistent with is its non-polar character and consequent low affinity for the TEG. The ETB sensitivity value is higher than expected; it should be comparable to the TOL sensitivity on the basis of the similarity in their structures and it should be lower than the IPA sensitivity on the basis of its relatively low polarity. We believe that the concentrations of ETB in the test atmospheres may have been underestimated. The low sensitivity value for PCE can be rationalized by a combination of its low polarity and its high density; that is, since the extent of film swelling is determined by the (condensed) volume, rather than the mass, of sorbed vapor, higher density analytes should give lower sensitivities.[8]

Consistent with the qualitative assessment presented above, the *RI* values of the VOCs had little or no apparent effect on sensitivity. Were it otherwise, the lower *RI* value of IPA would have reduced its sensitivity, and the higher *RI* value of PCE would have increased its sensitivity. The *swelling efficiency* is a potential co-factor that could not be quantitatively evaluated. The study by Steinecker, et al. estimated swelling efficiencies for C8 MPN films to be ~0.2 for aliphatic and chlorinated aliphatic hydrocarbons and alcohols, and ~0.3 for aromatic hydrocarbons.[8] Applying these factors, however, did not alter the order of relative sensitivities observed here.

The LOD for each analyte was estimated using linear regressions of peak height against injected mass ($r^2 > 0.97$ in all cases but HEP, which was 0.91). Disregarding the residual errors of the regression models, the LOD was defined as the 3σ/slope where σ is the standard deviation of the baseline ($\sigma = 0.514$ pm). LOD values ranged from 38 ng of ETB to 325 ng of HEP and are listed in Table 1.

Direct comparisons of LODs with those cited in previous studies of optical sensing with patterned-nanoparticle or MPN films are difficult owing to differences in testing conditions and specific analytes; as discussed previously,[25] LODs can be as sensitive to operating conditions as to the inherent response characteristics of a sensor. For steady-state exposures, LODs are typically expressed in terms of air concentrations, and values reported for VOCs of similar volatility as those tested here (e.g., toluene or m-xylene) on the basis of transmission measurements range from < 1 ppm[17] to > 100 ppm[11,26] or even higher.[16] For chromatographic detection, LODs must be expressed in terms of (injected) mass derived from peak-height sensitivities, which are often affected significantly by operating conditions (e.g., injection band width, flow rate, detector-cell volume). The only direct comparison possible with our data are those reported by Chen, et al., who fashioned a GC detector from an LED-probed spiral capillary coated on the interior with a random monolayer of surface-bound gold nanoparticles with some degree of citrate functionalization. They reported an LOD of 62 ng for m-xylene, which is roughly 2× our LOD for ethylbenzene. Thus, our device appears to offer a sensitivity advantage, and it is also orders of magnitude smaller and better designed for microsystem integration. Our own reflectance measurements of a solvent-cast C8-MPN film yielded an LOD of 200 ng for discrete injections of toluene vapor through a make-shift detector cell,[10] as compared to our values of 91 ng here.

These (un-optimized) LODs are about an order of magnitude or more higher than those we have obtained using MPN-coated chemiresistors or a PDMS-coated μOFRR as GC or μGC detectors,[2,25,36] But clearly, there are several options to pursue to try to enhance the sensitivity of the MPN-coated μOFRR sensor, including optimizing the thickness and uniformity of the MPN films for the TEG MPN as well as for other MPN monolayer functionalities, reducing surface

roughness to increase the Q factor of the resonator, and possibly reducing the thickness of the resonator wall to increase the fraction of the evanescent field penetrating the MPN film.

Conclusions

The results obtained from this first report of an MPN-coated WGM resonator for VOC sensing are very encouraging. Responses to VOCs are rapid, reversible, and proportional to the VOC concentration, and sensitivities are comparable to or higher than those reported previously for optical VOC sensing with MPN films. The sensor and associated source and detector hardware are small, require relatively little power to operate and can be efficiently packaged; these features coupled with the integrated fluidic and optical interconnections incorporated on-chip greatly facilitate assembly into μGC systems.

By design, this study used a longer wavelength probe of the MPN interface layer, which produced a WGM resonance the evanescent field of which was apparently able to penetrate well beyond the thickness of the MPN film. Accordingly, red shifts in λ_{WGM} were observed for all VOCs, indicative of a response mechanism dominated by swelling-induced changes in film thickness and relatively insensitive to *RI* changes in the film. Although this would logically impart greater sensitivity to the sensor, it would also reduce or eliminate the selectivity expected on the basis of RI differences among the VOCs.

The μOFRR resonance was quite sensitive to the morphology of the MPN film, which apparently varies with the monolayer functionalization and deposition method. Although we succeeded in obtaining a TEG MPN film of sufficient uniformity within the μOFRR cavity after re-deposition from ethanol, the Q-factor of the WGM resonance was rather low. Further work is

needed to optimize the film deposition methodology in order to sustain high Q-factor resonances with all MPNs that might be used as interface layers.

Additional future efforts will focus on probing nanoparticle coated devices at shorter wavelengths, closer to the LSPR maximum of the MPN film, by use of different laser sources. MPN films are known to give differentiable responses to VOCs when probed at multiple visible wavelengths,[9,11] however, this has not yet been demonstrated using an optical resonator. Coupling the WGM resonance to the nanoparticle film LSPR should increase the diversity of responses and, as a consequence, the selectivity of the sensor. Arrays of MPN-coated μOFRR sensors probed at several discrete wavelengths as compact μGC detectors can be envisioned.

Acknowledgments

The authors gratefully acknowledge the following individuals for their technical assistance: Gustavo Serrano for help with OFRR coating and Lindsay K. Wright for help with OFRR coating and nanoparticle synthesis. Primary funding was provided by Grant ECCS 1181257 and Grant ECCS 1128157 from the National Science Foundation. Additional funding was provided by a grant from Agilent Technologies. Devices were fabricated in the Lurie Nanofabrication Facility, a member of the National Nanotechnology Infrastructure Network, which is supported by the NSF**.**

References

1 H. Wohltjen and A. W. Snow, *Anal. Chem.*, 1998, **70**, 2856-2859.

2 C.-J. Lu, W. H. Steinecker, W.-C. Tian, M. C. Oborny, J. M. Nichols, M. Agah, J. A. Potkay, H. K. Chan, J. Driscoll and R. D. Sacks, S. W. Pang, K. D. Wise, and E. T. Zellers *Lab Chip*, 2005, **5**, 1123-1131.

3 X. Shi, L. Wang, N. Kariuki, J. Luo, C.-J. Zhong and S. Lu, *Sens. Actuators, B: Chem.*, 2006, **117**, 65-73.

4 R.-S. Jian, R.-X. Huang and C.-J. Lu, *Talanta*, 2012, **88**, 160-167.

5 F. I. Bohrer, E. Covington, Ç. Kurdak and E. T. Zellers, *Anal. Chem.*, 2011, **83**, 3687-3695.

6 J. W. Grate, D. A. Nelson and R. Skaggs, *Anal. Chem.*, 2003, **75**, 1868-1879.

7 K. Scholten, L. K. Wright and E. T. Zellers, *IEEE Sens. J.*, 2013, **13**, 2146-2154.

8 W. H. Steinecker, M. P. Rowe and E. T. Zellers, *Anal. Chem.*, 2007, **79**, 4977-4986.

9 R. A. Potyrailo, M. Larsen and O. Riccobono, *Angew. Chem. Int. Ed.*, 2013, **52**, 10360-10364.

10 K. Scholten, K. Reddy, X. Fan and E. T. Zellers, *Anal. Methods*, 2013, **5**, 4268-4272.

11 K.-J. Chen and C.-J. Lu, *Talanta*, 2010, **81**, 1670-1675.

12 F.-Y. Chen, W.-C. Chang, R.-S. Jian and C.-J. Lu, *Anal. Chem.*, 2014.

13 C.-S. Cheng, Y.-Q. Chen and C.-J. Lu, *Talanta*, 2007, **73**, 358-365.

14 M. C. Dalfovo, R. C. Salvarezza and F. J. Ibañez, *Anal. Chem.*, 2012, **84**, 4886-4892.

15 J. C. Love, L. A. Estroff, J. K. Kriebel, R. G. Nuzzo and G. M. Whitesides, *Chem. Rev.*, 2005, **105**, 1103-1170.

16 T. Karakouz, A. Vaskevich and I. Rubinstein, *J. Phys. Chem., B*, 2008, **112**, 14530-14538.

17 A. Monkawa, T. Nakagawa, H. Sugimori, E. Kazawa, K. Sibamoto, T. Takei and M. Haruta, *Sens. Actuators, B: Chem.*, 2014, **196**, 1-9.

18 B. Chen, C. Liu, M. Ota and K. Hayashi, *IEEE Sens. J.*, 2013, **13**, 1307-1314.

19 K. Reddy, Y. Guo, J. Liu, W. Lee, M. K. K. Oo and X. Fan, *Sens. Actuators, B: Chem.*, 2011, **159**, 60-65.

20 K. Reddy, Y. Guo, J. Liu, W. Lee, M. K. K. Oo and X. Fan, *Lab Chip*, 2012, **12**, 901-905.

21 Y. Sun and X. Fan, *Opt. Express*, 2008, **16**, 10254-10268.

22 Y. Sun, S. I. Shopova, G. Frye-Mason and X. Fan, *Opt. Lett.*, 2008, **33**, 788-790.

23 Y. Sun, J. Liu, D. J. Howard, G. Frye-Mason, A. K. Thompson, S.-j. Ja and X. Fan, *Analyst*, 2010, **135**, 165-171.

24 K. Scholten, X. Fan and E. T. Zellers, *Appl. Phys. Lett.*, 2011, **99**, 141108.

25 K. Scholten, X. Fan and E. T. Zellers, *Lab Chip*, 2014, **14**, 3873-3880.

26 C. Zhang, L. Wright, K. Scholten, X. Fan and E.T. Zellers, *Proc. 18th Int'n'l Conf. Solid-State Sensors, Actuators, Microsystems, Transducers '15,* Anchorage AK, June 21-25, 2015, accepted for publication.

27 M. P. Rowe, K. E. Plass, K. Kim, C. Kurdak, E. T. Zellers and A. J. Matzger, *Chem. Mater.*, 2004, **16**, 3513-3517.

28 G. Serrano, S. M. Reidy and E. T. Zellers, *Sens. Actuators, B: Chem.*, 2009, **141**, 217-226.

29 S. Reidy, D. George, M. Agah and R. Sacks, *Anal. Chem.*, 2007, **79**, 2911-2917.

30 Y. Wan, N. Goubet, P.-A. Albouy, N. Schaeffer and M.-P. Pileni, *Langmuir*, 2013, **29**, 13576-13581.

31 Y. Joseph, B. Guse, T. Vossmeyer and A. Yasuda, *J. Phys. Chem., C*, 2008, **112**, 12507-12514.

32 M. C. Dalfovo, L. J. Giovanetti, J. M. Ramallo-Lopez, R. C. Salvarezza, F. G. Requejo and F. J. Ibañez, *J. Phys. Chem., C*, 2015, DOI: 10.1021/jp511014q.

33 S. Kubo, A. Diaz, Y. Tang, T. S. Mayer, I. C. Khoo and T. E. Mallouk, *Nano Lett.*, 2007, **7**, 3418-3423.

34 Sigma-Aldrich, Triethylene glycol monomethyl ether properties, http://www.sigmaaldrich.com/catalog/product/aldrich/317292?lang=en&region=US, Accessed March 8th, 2015.

35 J. W. Grate, A. Snow, D. S. Ballantine, H. Wohltjen, M. H. Abraham, R. A. McGill and P. Sasson, *Anal. Chem.*, 1988, **60**, 869-875.

36 Q. Zhong, W. H. Steinecker and E. T. Zellers, *Analyst*, 2009, **134**, 283-293.

37 CRC Handbook of Chemistry & Physics, ed. D. R. Lide, CRC Press, Boca Raton, USA, 94th edn, 2013.

38 P. J. Linstrom and W. G. Mallard, eds., *WebBook, NIST Standard Reference Database Number 69*, National Institute of Standards and Technology, Gaithersburg, MD.

Table 1. Relevant physical properties and sensor response parameters of the analytes.[a]

VOC	ρ (g/ml)[b]	p_v (kPa)[c]	RI[b]	LOD (ng)[d]	FWHM (s)[d]	$FWHM_{FID}$ (s)[e]	FWHM ratio
IPA	0.781	5.64	1.378	75	0.83	0.72	1.2
HEP	0.680	5.97	1.386	320	1.0	0.81	1.2
TOL	0.862	3.76	1.494	91	1.7	1.1	1.5
PCE	1.623	2.46	1.506	150	2.2	1.5	1.5
ETB	0.863	1.25	1.493	38	3.3	2.2	1.5

[a] refractive index (*RI*), density (ρ), and vapor pressure (p_v) at 25 °C; [b] ref. 37; [c] ref. 38; [d] see Figure 4 for chromatographic conditions under which these values were obtained; [e] separation performed with same µcolumns as µOFRR separations and similar conditions such that retention times were identical.

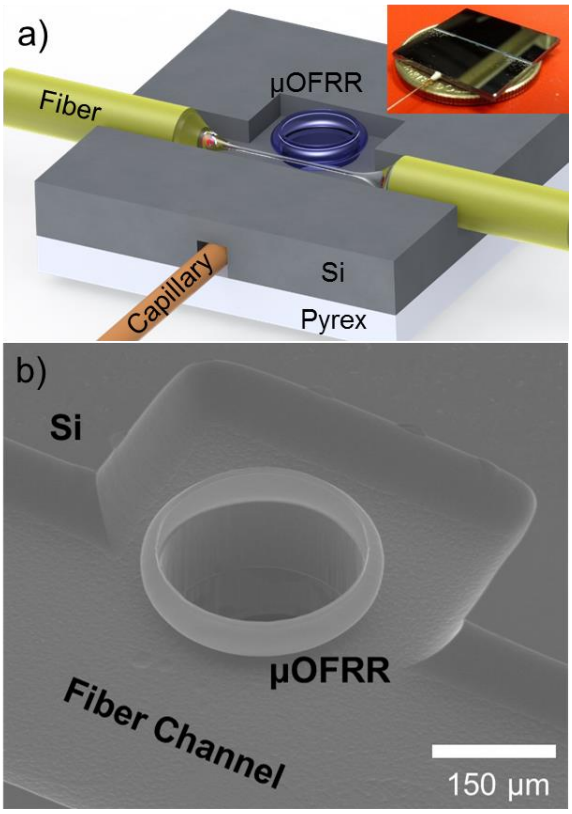

Figure 1. (a) Diagram of the μOFRR with attached optical fiber and capillary connection (inset shows a photograph of the fully packaged device); (b) SEM image of the μOFRR, with 250 μm i.d. and 1.2 μm thick walls.

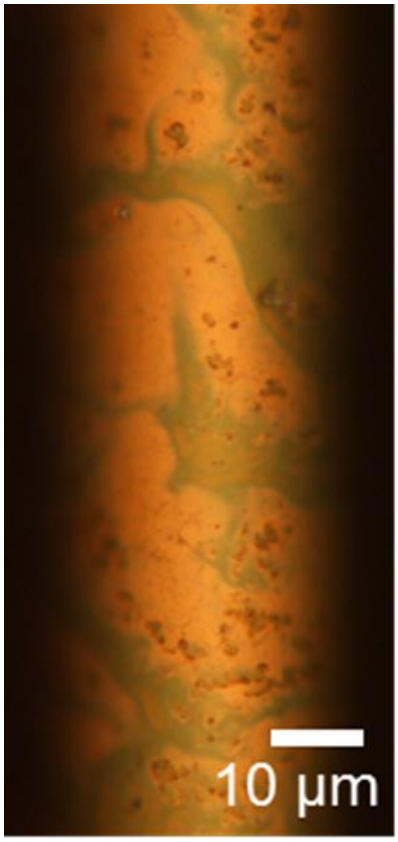

Figure 2. Dark-field optical microscope image of drawn-capillary OFRR with C8 MPN coating showing the non-uniformity of the C8 MPN film.

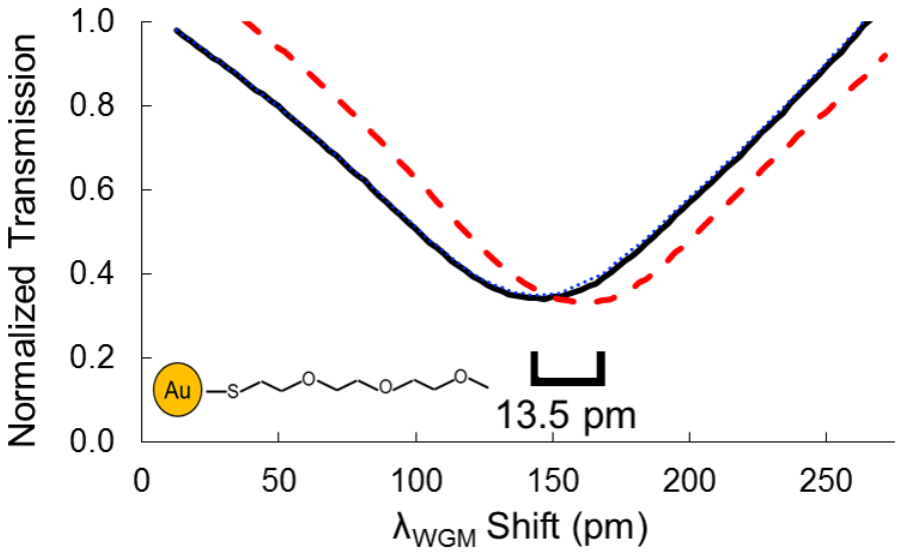

Figure 3. WGM resonance (1550 nm) observed in a TEG-MPN coated μOFRR sensor downstream from μGC separation columns during exposure to dry air carrier gas (black, solid line), 1.3 μg injection of ethylbenzene vapor (red, dashed line), and recovery after purging with dry air (dotted, blue line). Inset shows the structure of the TEG monolayer.

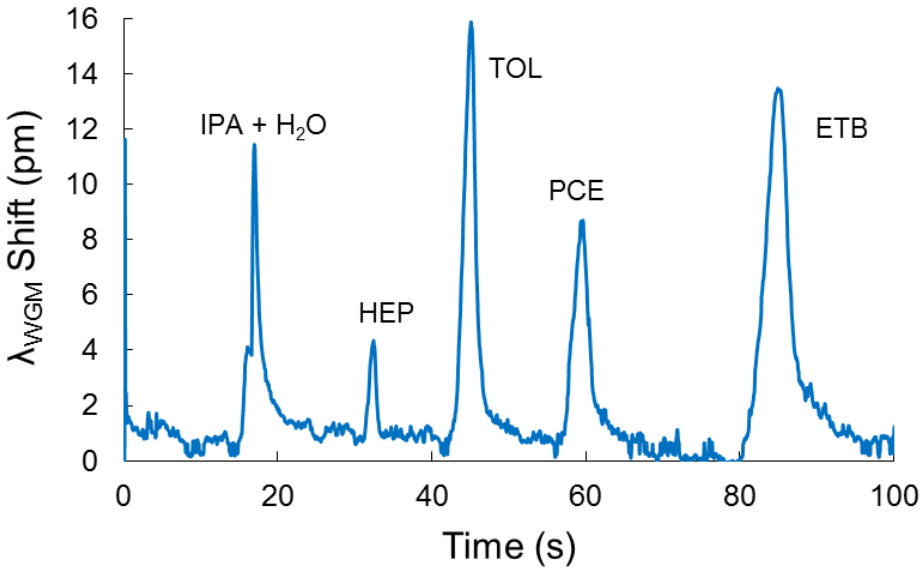

Figure 4. μGC separation of five VOCs with the TEG-coated μOFRR detector. The two series coupled μcolumn chips (each with a 3-m long PDMS coated separation channel) were at 40 °C and the downstream μOFRR sensor was at 22 °C. The dry-air carrier gas flow rate was 2.0 mL min^{-1}. Injected masses were approximately 1.2 μg IPA, 2.0 μg HEP, 2.5 μg TOL, 2.4 μg PCE, and 1.3 μg ETB. Note that IPA and background water vapor co-elute.

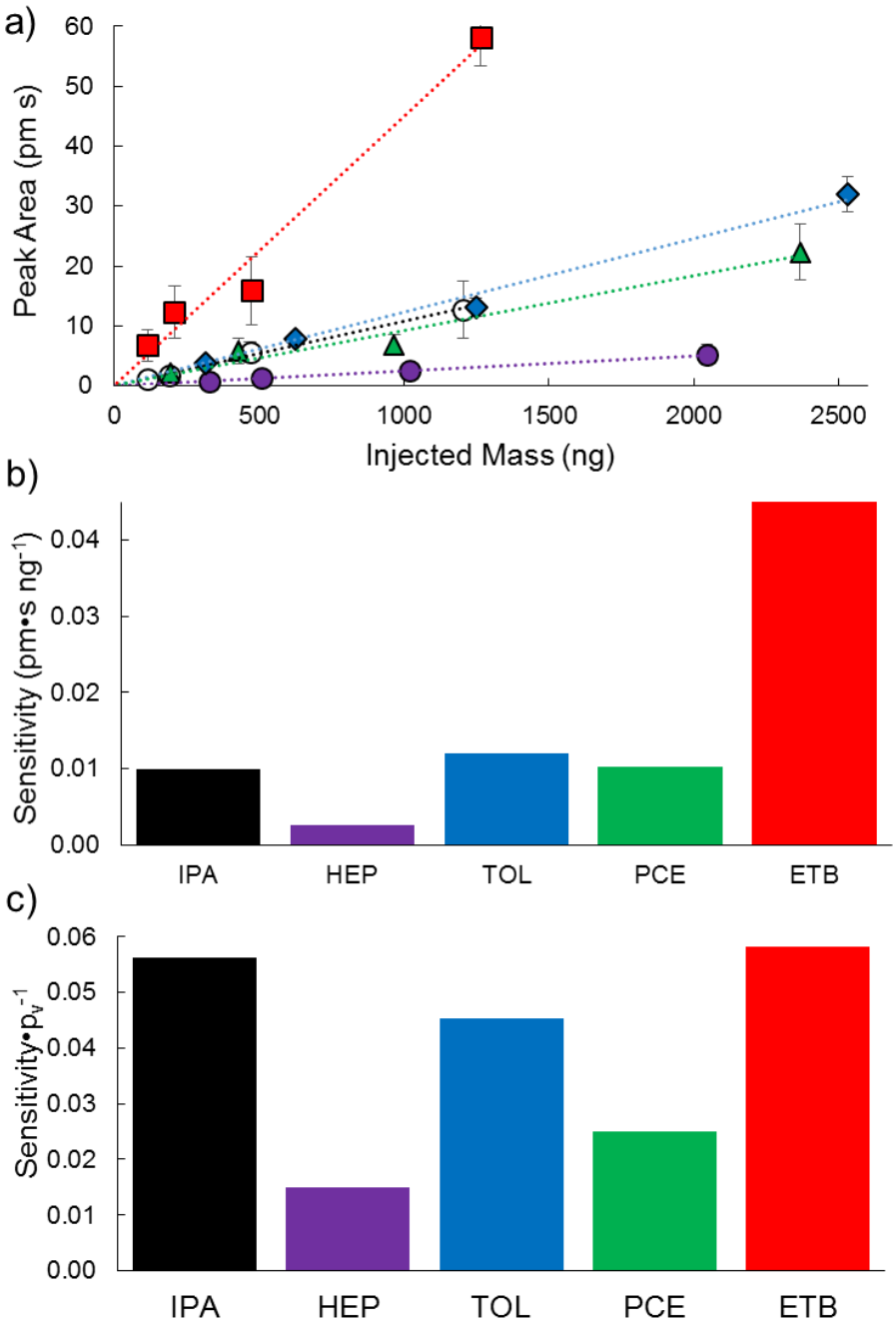

Figure 5. (a) TEG-coated µOFRR calibration curves (R^2 > 0.966 in all cases) for HEP (filled circles), PCE (triangles), IPA (unfilled circles), TOL (diamonds), and ETB (squares); (b) sensitivities derived from (forced-zero) regression slopes; (c) sensitivities normalized by analyte vapor pressures (kPa). Error bars in (a) represent +/- one standard deviation (n = 5 replicates). Note: the area of the H_20 peak co-eluting with the IPA peak was constant over the calibration range; it was determined from blank analyses and subtracted prior to plotting the data above.

Table of Contents image and text:

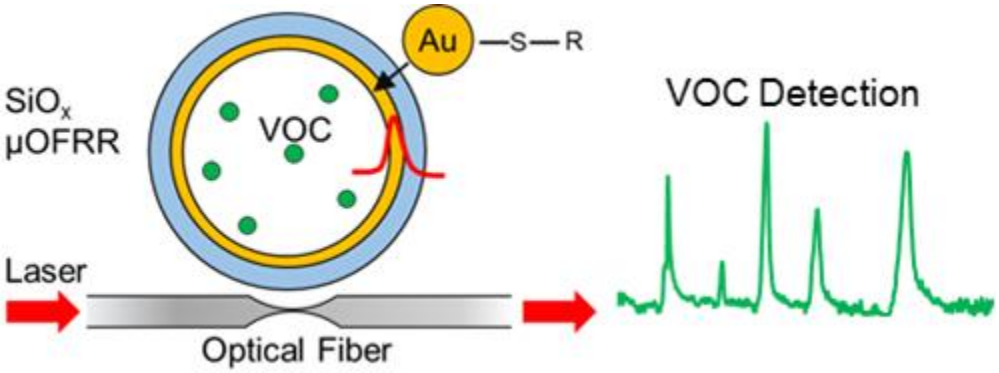

A microfabricated optofluidic ring resonator (μOFRR) sensor with a monolayer-protected nanoparticle interface layer is introduced and evaluated as a detector for micro-scale gas chromatography.